HHS Public Access

Author manuscript

Neuropharmacology. Author manuscript; available in PMC 2022 November 01.

Published in final edited form as:

Neuropharmacology. 2022 November 01; 218: 109233. doi:10.1016/j.neuropharm.2022.109233.

Peroxisome proliferator-activated receptor gamma agonist ELB00824 suppresses oxaliplatin-induced pain, neuronal hypersensitivity, and oxidative stress

Morgan Zhang[a,b,c,d,1], **Min Hu**[d,1], **Sascha R.A. Alles**[e], **Marena A. Montera**[e], **Ian Adams**[e], **Maria D. Santi**[a,b], **Kenji Inoue**[a,b], **Nguyen Huu Tu**[a,b], **Karin N. Westlund**[e], **Yi Ye**[a,b,*]

[a]Bluestone Center for Clinical Research, New York University College of Dentistry, 421 First Avenue, 233W, New York, NY, 10010, USA

[b]Department of Molecular Pathobiology, New York University College of Dentistry, 345 E. 24th street, New York, NY, 10010, USA

[c]USA Elixiria Biotech Inc, Hartsdale, NY, 10530, USA

[d]Shanghai Elixiria Biotech Co. Ltd, 578 Yingkou Road, Yangpu District, Shanghai, 200433, China

[e]Department of Anesthesiology & Critical Care Medicine, MSC10 6000, 2211 Lomas Blvd. NE, University of New Mexico Health Sciences Center, Albuquerque, NM, 87131, USA

Abstract

Chemotherapy-induced neuropathic pain (CINP) is a debilitating and difficult-to-treat side effect of chemotherapeutic drugs. CINP is marked with oxidative stress and neuronal hypersensitivities. The peroxisome proliferator-activated receptor gamma (PPARγ) is a transcription factor that regulates genes involved in oxidative stress and inflammation. We hypothesize that PPARγ agonists are protective against CIPN by reducing oxidative stress and inhibiting neuronal hypersensitivities. To test our hypothesis, acute or chronic CIPN was introduced by short or long-term treatment of oxaliplatin in BALB/c mice. CIPN mice were treated with either a novel blood-brain barrier (BBB) penetrable PPARγ agonist ELB00824, or a BBB non-penetrable PPARγ agonist pioglitazone, or vehicle. Cold allodynia, mechanical allodynia, motor coordination, sedation and addiction were measured with dry ice, von Frey filaments, beam-walking tests, and

*Corresponding author. Bluestone Center for Clinical Research, New York University College of Dentistry, 421 First Avenue, 233W, New York, NY, 10010, USA. yy22@nyu.edu (Y. Ye).

[1]Morgan Zhang and Min Hu contributed equally to the project.

Declaration of competing interest

The authors declare that they have no competing financial interests that could have appeared to influence the work reported in this paper other than that KNW is a scientific advisory board member of the USA Elixiria Biotech Inc., and MZ is a funder of both Shanghai Elixiria Biotech Inc. and USA Elixiria Biotech Inc.

CRediT authorship contribution statement

Morgan Zhang: Conceptualization, Data curation, Formal analysis, Funding acquisition, Investigation, Methodology, Project administration, Resources, Supervision, Validation, Visualization, Writing – original draft, Writing – review & editing. **Min Hu:** Investigation, Data curation. **Sascha R.A. Alles:** Conceptualization, Funding acquisition, Methodology, Resources, Supervision, Writing – review & editing. **Marena A. Montera:** Investigation, Data curation. **Ian Adams:** Investigation, Data curation. **Maria D. Santi:** Investigation, Data curation. **Kenji Inoue:** Technical support. **Nguyen Huu Tu:** Technical support. **Karin N. Westlund:** Conceptualization, Funding acquisition, Methodology, Resources, Supervision, Writing – review & editing. **Yi Ye:** Conceptualization, Funding acquisition, Formal analysis, Methodology, Project administration, Resources, Supervision, Validation, Visualization, Writing – original draft, Writing – review & editing.

conditioned place preference, respectively. Oxidative stress was accessed by measuring byproducts of protein oxidation (carbonyl and 3-Nitrotyrosine) and lipid peroxidation [Thiobarbituric acid reactive substances (TBARS)], as wells as gene expression of *Cat*, *Sod2*, *Ppargc1a*. The effects of ELB00824 on nociceptor excitability were measured using whole-cell electrophysiology of isolated dorsal root ganglion neurons. Preemptive ELB00824, but not pioglitazone, reduced oxaliplatin-induced cold and mechanical allodynia and oxidative stress. ELB0824 suppressed oxaliplatin-induced firing in $IB4^{-}$ neurons. ELB00824 did not cause motor discoordination or sedation/addiction or reduce the antineoplastic activity of oxaliplatin (measured with an MTS-based cell proliferation assay) in a human colon cancer cell line (HCT116) and a human oral cancer cell line (HSC-3). Our results demonstrated that ELB00824 prevents oxaliplatin-induced pain, likely via inhibiting neuronal hypersensitivities and oxidative stress.

Keywords

Chemotherapy-induced neuropathy; Oxaliplatin; PPAR; Non-addictive; Neuropathic pain; Oxidative stress

1. Introduction

Chemotherapy-induced peripheral neuropathy (CIPN) is one of the most frequent adverse events caused by cancer therapeutics. While oxaliplatin, a third-generation novel platinum-derived compound, has acquired significant results in the treatment of advanced metastatic colorectal cancer, ovarian, breast, and lung cancer, it has a serious side effect characterized by paresthesia and dysesthesia of hands and feet, resulting in discontinuation of the therapy[1]. Treatment options for oxaliplatin induced CIPN are very limited, with only moderate evidence for pain relief provided by duloxetine - a selective serotonin and norepinephrine reuptake inhibitor antidepressant (SSNRI) in clinical trials (Zajączkowska et al., 2019). Therefore, understanding the mechanism of action and developing novel treatments for CIPN is a clinically meaningful and pressing need.

The mechanisms underlying the development of CIPN are related to oxidative stress, mitochondrial dysfunction, and neuroinflammation at the periphery as well as at the central nervous system (Ma et al., 2018). The nervous system is especially susceptible to chemotherapy-induced oxidative damage, and strategies targeting oxidative stress have been extensively studied to treat CIPN. However, most strategies targeting oxidative stress are by external antioxidant supplementation; their efficacy for CIPN in clinical studies is not satisfying (Hu et al., 2019). An alternative strategy is to boost endogenous antioxidant responses. PPARγ has emerged as a central hub in endogenous responses against oxidative stress. PPARγ is activated by a variety of endogenous fatty acid derived compounds (*e.g.*, palmitoylethanolamide) and the thiazolidinediones (TZD) class of diabetes drugs (*e.g.*, pioglitazone and rosiglitazone) (Quintão et al., 2019). Upregulation of key antioxidant enzymes, including Superoxide dismutase (*Sod*), glutathione peroxidase, PPARγ coactivator 1 - alpha (*Ppargc1a*), catalase (*Cat*), and enhanced mitochondrial energy metabolism, have been observed upon PPARγ activation. In addition, PPARγ agonists have been shown to attenuate neuronal hypersensitivity by suppressing immune responses activated by ROS

accumulation, underscoring the importance of therapeutic strategies that suppress oxidative stress (Khasabova et al., 2019).

However, PPARγ agonists exhibit mixed results against CIPN, despite their protective effects against neurotoxicity induced by chemotherapy (Alsalem et al., 2019; Khasabova et al., 2019). Rosiglitazone failed to suppress oxaliplatin-induced cold hyperalgesia and spinal oxidative stress in an animal model of CIPN (Jain et al., 2011). In a clinical trial using palmitoylethanolamide for CIPN, no beneficial effect was observed against small fiber injury (Truini et al., 2011). A possible explanation towards the less-than-optimal effect of all current PPARγ agonists on CIPN is their low blood brain barrier (BBB) permeability, which prevents them from achieving the minimal effective concentration in the CNS (Westlund and Zhang, 2020; G et al., 2021). By far, most research examining the underlying mechanisms of CIPN have been concentrated on those occurring in the PNS. However, a growing body of evidence underscores the importance of the CNS in CIPN (Boland et al., 2014; Li et al., 2015). Chemotherapeutics can produce adverse effects on the human brain, evidenced by cognitive impairment and abnormal pain processing in the CNS (Boland et al., 2014). Oxaliplatin administered systemically can cross the BBB, sensitizing the spinal cord neurons to produce hyperalgesia, whereas the hindpaw injection of oxaliplatin, which is peripherally restricted, does not produce hyperalgesia at the relevant doses (Huang et al., 2016).

We hypothesize that BBB permeable PPARγ agonists that are neuroprotective for both peripheral nerves and the CNS could be more effective in minimizing CIPN. We have synthesized a series of BBB permeable PPARγ agonists, including a highly BBB permeable PPARγ agonist ELB00824. ELB00824 and the marketed diabetic drug pioglitazone exhibit similar *in vitro* potency for the transcription of genes downstream to PPARγ activation (Zhang et al., 2019). However, due to its higher BBB permeability (Westlund and Zhang, 2020; Truini et al., 2011), ELB00824 but not pioglitazone can significantly increase PPARγ expression in the medullary spinal trigeminal subnuclei (Lyons et al., 2017). In a trigeminal neuropathy model, ELB00824 exhibits superior therapeutic window than pioglitazone (Westlund and Zhang, 2020).

In the present study, we examined whether our highly BBB permeable PPARγ agonist ELB00824 is a better candidate for oxaliplatin-induced peripheral neuropathy (OIPN) prevention and treatment than a low BBB permeable PPARγ agonist pioglitazone using both acute and chronic oxaliplatin treatment models. In addition, we explored the mechanism of action of ELB00824 on neuronal oxidative stress and peripheral neuronal hypersensitivity induced by oxaliplatin. Finally, we evaluated the safety of ELB00824 by testing its effect on motor coordination, sedation/addiction, and antineoplastic activity of oxaliplatin.

2. Materials and methods

2.1. Materials

ELB00824 was synthesized as described previously (Zhang et al., 2019). All other chemicals were purchased from Sigma-Aldrich (St. Louis, MO), including duloxetine hydrochloride (CAS: 116539-59-4), oxaliplatin (CAS: 61825-94-3), pioglitazone hydrochloride (PPARγ agonist, CAS: 112529-15-4), T0070907 (a potent and selective

PPARγ antagonist, CAS: 313516-66-4), and Cremophor@EL (CAS: 61791-12-6). Oxaliplatin was dissolved in 5% glucose solution. ELB00824 and pioglitazone were dissolved in DMSO/Cremophor vehicle [30% DMSO and 15% Cremophor@EL in phosphate buffered saline (PBS) buffer (pH 7.4)], and vortexed for 30 s before administration. T0070907 was dissolved in DMSO to make stock solution of 66 mg/ml, and then dissolved into saline to make solution of 2.0 or 4.0 mg/ml for intrathecal (i.t.) or intraperitoneal (i.p.) injection, respectively.

2.2. Animals

This study was approved by the Institutional Animal Care and Use Committees of New York University and the University of New Mexico Health Sciences Center. Female and male BALB/c mice (8–12 weeks old) were housed in a temperature-controlled room on a 12:12 h light cycle (06:00–18:00 h light), with unrestricted access to food and water. All animals were acclimated for at least 1 week before the experiments and randomly assigned to treatment groups. The experimenters were blinded to the treatment groups whenever possible.

2.3. Cell culture

Human colorectal carcinoma cells (HCT116) (ATCC, Manassas, Virginia), and human oral squamous carcinoma cells (HSC-3) (passage 4–10, Japanese Collection of Research Bioresources, Osaka, Japan) were grown in DMEM (Invitrogen) containing antibiotic (penicillin/streptomycin, 10 U/ml) and 10% fetal bovine serum (FBS). Human embryonic kidney cells (HEK293) were purchased from ATCC and grown in DMEM medium containing 10% FBS. All cells were cultured in a humidified atmosphere containing 5% CO2 at 37 °C. Cells were authenticated by ATCC and routinely tested for Mycoplasma (PlasmoTest Mycoplasma Detection Kit; InvivoGen).

2.4. In vitro antioxidative effects of ELB00824

The antioxidative potencies (EC_{50}) of oxidative stress was measured in HEK293 cells using the ROS-Glo™ H_2O_2 assay (Promega, Madison, WI). HEK293 cells were cultured in 96-well plates at a density of 5000 cells per well in 70 μl of the DMEM medium for 6 h, and then 5 μl vehicle (0.5% v/v DMSO) or test compounds (ELB00824, rosiglitazone, pioglitazone) were added into each well with final concentrations of 0.3, 1, 3, 10, 30 μM. Eighteen hours later, 20 μl of H_2O_2 substrate solution was added to the cells and incubated for 6 h at 37 °C in a 5% CO_2 incubator. Then, 50 μl of culture medium from each well was transferred to new wells of a white 96 well plate (Thermo Fisher, Waltham, MA), and mixed with 50 μl of ROS-Glo™ Detection Solution. After additional 20 min incubation at room temperature, relative luminescent values (RLU) were recorded using a GloMax® Multi Detection System luminometer (Promega, Madison, WI). Inhibition of ROS production was calculated using the following equation: Inhibition ratio (%) = [1− RLU (compound-treated cells)/RLU (Control)] × 100%. The EC_{50}, E_{max} and standard errors for each parameter for inhibition of ROS production were calculated using Prism 9 statistics software based on the following equations: Sigmoidal, Sigmoid, 4 Parameter, $f = y0 + a/(1 + \exp(-(x-x_0)/b))$, where $a = E_{max}$, b = slope and $x_0 = EC_{50}$.

2.5. Preventative effect of ELB00824 in an acute model of OIPN

Oxaliplatin (5% glucose liquid solution; 3 mg/kg) was delivered i.p for 5 consecutive days with cumulative dosages of 15 mg/kg (Pozzi et al., 2020; Warncke et al., 2021), equivalent to a total human equivalent dose (HED) of 555 mg/m^2 (considering the K_m factor 37 for the conversion of animal doses to the Human Equivalent Dose; Nair and Jacob, 2016). ELB00824 was i.p. administered 5 min before oxaliplatin injection at the dose of 0, 3, 10, or 30 mg/kg. The vehicle control group received DMSO/Cremophor mixture injection 5min before 5% glucose solution injected via i.p. To determine whether ELB00824 treatment alone induces behavioral changes, we injected mice with a high dose of ELB00824 (30 mg/kg) without oxaliplatin treatment. All treatments of chemicals or vehicles were given every day in the morning for 5 consecutive days. Eight animals were used per group. Behaviors related to cold hyperalgesia and mechanical allodynia were measured at the baseline and on the 1st day after the 5-day treatment schedule (Fig. 1).

2.6. Preventative and treatment effect of ELB00824 in a chronic model of OIPN

Oxaliplatin mixed in 5% glucose liquid solution was delivered intravenously (i.v.) via the tail vein using a dose of 5 mg/kg twice per week for 4 consecutive weeks with cumulative dosages of 40 mg/kg (Pozzi et al., 2020), equivalent to a total HED of 1480 mg/m^2 (Nair and Jacob, 2016). To determine the preventative effect of ELB00824 on OIPN, ELB00824 was i.p. administered 5 min before oxaliplatin injection at the dose of 0, 3, 10, or 30 mg/kg. The vehicle control group received DMSO/Cremophor mixture injection 5min before i.v. injection of 5% glucose solution. To determine whether ELB00824 treatment alone induces behavioral changes, we injected mice with a high dose of ELB00824 (30 mg/kg) without oxaliplatin treatment. Six groups (n = 20/group) were used. Half of the animals were sacrificed at the end of week 4 for tissue on the 3rd day after last dosing (lumbar spinal cords) collection, and the remaining mice were observed for a follow-up period of another 4 weeks. The tissue was snap frozen in liquid nitrogen and stored at −80 °C. Behaviors related to cold and mechanical allodynia were measured at the baseline, at the end (the 3rd day after last dosing) of 4 week-treatment period, or at the end of 4-week follow-up period (Fig. 1).

To determine the acute treatment effect of ELB00824 on OIPN we used another 4 groups of mice (n = 8/group). Mice were treated with DMSO/Cremophor vehicle or three doses of ELB00824 (3, 10, 30 mg/kg) via i.p. on the 3rd day following the 4-week treatment schedule of oxaliplatin. Cold hyperalgesia and mechanical allodynia were measured at the baseline before oxaliplatin treatment, −1, 1, and 2 h after ELB00824 or vehicle injection (Fig. 1).

To compare the preventative analgesic effect between ELB00824 and pioglitazone and determine whether their effect is mediated centrally, we used another 5 groups of mice (n = 8/group) using the chronic OIPN model. 5 min before each bi-weekly oxaliplatin injection, mice received i.p. injection of either 30 mg/kg pioglitazone, a PPARγ antagonist T0070907 (30 mg/kg), or the DMSO/Cremophor vehicle 5 min before ELB00824 i.p. treatment (Fig. 1).

2.7. Measurement of mechanical allodynia and cold hyperalgesia

Animals were acclimated for 60 min before the initiation of behavior tests. To assess mechanical thresholds, mice were placed on an elevated mesh grid, where the paw withdraw threshold was measured with a set of von Frey filaments (0.07–8 g, Stoelting, Wood Dale, IL). Fifty percent mechanical withdrawal threshold (MWT) values were determined using the up-down method (Chaplan et al., 1994). Cold hyperalgesia was measured using a well-established protocol with dry ice (Brenner et al., 2012) at the right hind paw. Mice were kept in a restrainer box on a clear glass sheet (with 3/32 inch in thickness). Mice were tested by extending the tip of a dry ice pellet past the end of a syringe pressing to the glass underneath the hindpaw with light but consistent pressure. The withdrawal latency was measured with a stopwatch. Withdrawal was defined as any action to move the paw vertically or horizontally away from the cold glass. The maximum time allowed for withdrawal was 20 s to avoid potential tissue damage.

2.8. Whole-cell patch-clamp electrophysiology from dorsal root ganglia (DRG) cultures

DRGs from all levels from 6 naïve male mice were isolated, acutely dissociated and cultured for whole-cell patch-clamp electrophysiology as described previously (Goins et al., 2022). Briefly, collected DRG was digested using dispase II and collagenase type 2. Cells were grown in DMEM medium (10% fetal bovine serum, 1% antibacterial/antimycotic) and incubated at 37 °C, 5% CO_2 until use. Neurons were identified by infrared differential interference contrast (IR-DIC) connected to an Olympus digital camera. Current clamp recordings were performed using a Molecular Devices Multiclamp 700B (Scientifica, UK). Signals are filtered at 5 KHz, acquired at 50 KHz using a Molecular Devices 1550B converter (Scientifica, UK) and recorded using Clampex 11 software (Molecular Devices, Scientifica, UK). Electrodes were pulled with a Zeitz puller (Werner Zeitz, Martinsreid, Germany) from borosilicate thick glass (GC150F, Sutter Instruments). The resistance of the electrodes, following fire polishing of the tip, range between 5 and 8 MΩ. Bridge balance is applied to all recordings. Intracellular solution contains (in mM) 125 K-gluconate, 6 KCl, 10 HEPES, 0.1 EGTA, 2 Mg-ATP, pH 7.3 with KOH, and osmolarity of 290–310 mOsm. Artificial cerebrospinal fluid (aCSF) contains (in mM) 113 NaCl, 3 KCl, 25 $NaHCO_3$, 1 NaH_2PO_4, 2 $CaCl_2$, 2 $MgCl_2$, and 11 D-glucose. IB_4^+ and $IB4^-$ neurons have distinct functional roles in pain pathophysiology (Stucky and Lewin, 1999; Fang et al., 2006; Noh et al., 2019). Therefore, we recorded from small (<30 μm) IB_4^+ and IB_4^- neurons. The green fluorescent Alexa Fluor™ 488 isolectin GS-IB4 conjugate (Invitrogen, Eugene, OR, USA) (5 μg/ml) was applied to DRG neurons in culture media for 10 min prior to recording. IB_4^+ neurons display green fluorescence and only the brightest neurons will be considered $IB4^+$ to avoid misclassification. Cultures were treated with ELB00824 (10 μM) with or without oxaliplatin (50 μM) or vehicle (0.1% DMSO for ELB00824 or water for oxaliplatin) for 1 h prior to recording.

2.9. Measurement of oxidative stress markers

Mouse spinal cords of the lumbar region (n = 5/group) collected on the 3rd day after last dosing from chronic model of OIPN were homogenized by a Potter-Elvehjem homogenizer

in 10 mL PBS with 1 mM EDTA, and then centrifuged at 600×*g* for 10 min at 4 °C. Supernatant was collected and centrifuged again at 10,000 g for 10 min at 4 °C. Total protein of each supernatant sample was quantified using a BCA Protein Assay Kit (Pierce, Rockford, IL, USA). Lipid peroxidation was estimated by measuring the TBARS level (Okhawa et al., 1979). The absorbance of the TBARS was measured at 532 nm and quantified in nmole/milligram of total protein using 1,1,3,3-tetramethoxypropane as the standard. Lipid peroxidation (TBARS), protein oxidation (carbonyl group) and nitration (3-nitrotyrosine moiety) concentration in the supernatant were measured using a GloMax-Multi Detection System (Promega, Madison, USA). 3-nitrotyrosine content in the spinal cord tissue homogenates was determined with the aid of the 3-Nitrotyrosine ELISA kit (Ab116691; Abcam, Cambridge, MA, USA). Protein carbonylated group level was determined with an assay (Colombo et al., 2016) involving derivatization with 2,4-dinitrophenylhydrazine (DNPH). All samples were measured in triplicates and the absorbance was read using a GloMax-Multi Detection System (Promega, Madison, USA). All concentration was normalized to the total protein concentration of each sample.

2.10. Quantitative real-time polymerase chain reaction with reverse transcription (qRT-PCR)

DRGs (L3–L4) and Spinal cords were isolated from mice following 5-day treatment regimen (as described in section 2.5) with Oxaliplatin (n = 6), Oxaliplatin + ELB00824 (30 mg/kg, n = 6), and Oxaliplatin + pioglitazone (30 mg/kg, n = 5), and subjected to RNA extraction using TRIzol Reagent™ (Invitrogen, #15596026). Reverse transcription was performed using a High-capacity cDNA kits according to the manufacturer's instructions (ThermoFisher Scientific, #4368814). qPCRs were carried out in a AriaMx (Agilent) using PowerUp™ SYBR™ Green Master Mix (Applied Biosystems Inc., #A25741). Mouse primers were purchased from Life Technologies: *Cat* (*reverse*) GTGTGCCATCTCGTCAGTGAA, *Cat* (*forward*) GGAGGCGGGAACCCAATAG; Sod2 (*reverse*) TGTGTGGCTCCAGCGCGCCA, *Sod2* (*forward*) ATGTTGTGTCGGGCG GCGTG; *Ppargc1a* (*reverse*) CCACTTCAATCCACCCAGAAAG, *Ppargc1a* (*forward*) TATGGAGTGACATAGAGTGTGCT; *Pparg* (*reverse*) AATCCTT GGCCCTCTGAGAT, Pparg (*forward*) TTTTCAAGGGTGCCAGTTTC. The housekeeping gene *Gapdh* was used as the internal control gene. Analyses were carried out in triplicate, and the relative quantification of gene expression data was calculated using the 2−ΔΔCt method.

2.11. Beam-walking tests

Motor performance was measured with a beam-walking test and an inclined balance beam apparatus (Marmiroli et al., 2017). On day 1, all animals completed five unassisted runs across the entire length of the beam. On day 2, 2 h after i.p. injection of vehicle, 30 mg/kg of carbamc0020 … azepine (positive control) or 10, 30, 60,90, 120 mg/kg of ELB00824 (n = 6), all animals were transferred to the start of the balance beam, and required to run five trials. Sixty seconds were allotted for each trial. Latency and Number of errors were recorded. Latency is the time that was required for the animal to reach the goal box. Failure to reach or falling from the beam was scored as a latency of 60 s. Any failed attempt to hold onto the beam with either extremities or the tail, any loss of balance, or any fall from the

beam before end of the 60 s assigned to each assay were counted and recorded as number of errors.

2.12. Conditioned place preference (CPP)

The CPP test performed using a two-compartment box (Maldonado et al., 1997). Eight groups of mice (n = 3) were assigned to this study. To pair the drug with one of two distinct contexts, each group was assigned a 'side' of the addiction box: blank or striped. Mice assigned to the blank side would be placed in the blank chamber after receiving their injection; mice assigned to the striped side would be placed in the striped chamber after receiving their injection. Mice were also assigned i.p. injection of either vehicle, morphine (5 mg/kg), ELB 30 or 60 (ELB00824, 30 or 60 mg/kg). Thus, the groups were as follows: (1) Vehicle-Blank, (2) Vehicle-Striped, (3) morphine-Blank, (4) morphine-Striped, (5) ELB 30-Blank, (6) ELB 30-Striped, (7) ELB 60-Blank, (8) ELB 60-Striped. Mice were screened for initial preferences on the morning of day 1 by placing mice in the small central space and allowing them to move freely throughout the entire apparatus for 15 min while recording time spent (pre-conditioning) in the two outer chambers. For the subsequent three days, mice were injected with their assigned drug and placed in their assigned chamber, without access to the other chamber, for 30 min. On the fifth day, mice were placed in the middle of the box and allowed access to both chambers for 15 min. Then post-conditioning time spent (post-drug) in each chamber was recorded, and the group mean was calculated. Data were plotted as the difference in the time spent on the drug-paired side before training subtracted from the times spent on the drug-paired side after training.

2.13. Cytotoxicity assay

Cytotoxicity and cell viability were assessed using a CellTiter 96® AQ_{ueous} One Solution Cell Proliferation Assay (Promega, Madison, WI). HCT116 or HSC-3 cells were seeded at a density of 7500, 3000, 10000 cells/well, respectively, onto 96-well microtiter plates with 100 μl culture medium, In the following day, oxaliplatin and ELB00824 were dissolved in deionized water with 1% ethanol. Cells were exposed to oxaliplatin (0.3, 1, 3, 10, 30, 60 μM) and ELB00824 (0, 10, 30 μM). Forty-eight hours later, 20 μL CellTiter 96® AQ_{ueous} One Solution Reagent was added to each well, and the plates were incubated for 2 h at 37 °C in a humidified, 5% CO_2 incubator. The absorbance was then read at 490 nm using a GloMax-Multi Detection System (Promega, Madison, USA).

2.14. Statistical analysis

We used Prism 9 statistics software package (GraphPad Software LLC, San Diego, CA) for all data analysis. Student's t-test was used for two-group analysis. One-way ANOVA or Kruskal–Wallis test with Dunnett's post hoc analysis were used to compare multiple groups. Two-way ANOVA with one within-subject factor (time) and one between-subject factor (treatment) followed by Holm-Sidak posthoc tests was used to compare the effect of different treatments over time. $P < 0.05$ was considered statistically significant. Results were presented as mean ± standard deviation (SD) or, if specified, standard error of the mean (SEM).

3. Results

3.1. Efficacy of ELB00824 on oxaliplatin-induced pain-like behaviors

In the acute OIPN model (Fig. 2A–D), oxaliplatin induced significant cold hyperalgesia and mechanical allodynia as predicted. ELB00824 treatment prevented oxaliplatin induced cold hyperalgesia and mechanical allodynia in a dose-dependent manner. No difference in cold hyperalgesia or mechanical allodynia was observed between mice treated with oxaliplatin alone or with 3 mg/kg ELB00824; the strongest preventative effect on oxaliplatin induced cold hyperalgesia and mechanical allodynia was observed with the highest ELB00824 dosing (30 mg/kg). No sex difference was observed in OIPN, or in response to ELB00824 during the observation period.

In the chronic OIPN model, at the end of 4-week oxaliplatin treatment, mice developed both cold and mechanical hypersensitivity (Fig. 2E–F). Again, we observed a dose-dependent effect of ELB00824 preemptive treatment on OIPN. The low dose (3 mg/kg) ELB00824 treatment was not effective, but both the 10 mg/kg and 30 mg/kg doses were effective in reducing oxaliplatin induced cold hyperalgesia and mechanical allodynia. The Minimal Effective Dose (MED) of ELB00824 on this mouse OIPN model is therefore around 10 mg/kg. To determine the long-lasting effect of chronic oxaliplatin or ELB00824 on cold hyperalgesia and mechanical allodynia, we observed mice for additional 4 weeks. Neither oxaliplatin nor ELB00824 treatment resulted in long-lasting effect on cold or mechanical hypersensitivities; no significant group difference was found (Fig. 2G and H).

In the chronic OIPN model, we also tested the acute treatment effect of ELB00824. At the end of 4-week oxaliplatin treatment, mice were given a single injection of ELB00824 with one of the three doses (3 mg/kg, 10 mg/kg, or 30 mg/kg). 30 mg/kg ELB00824, at 1 h following injection, significantly reversed both cold hyperalgesia and mechanical allodynia induced by chronic oxaliplatin treatment, but the effect was lost at 2 h following ELB00824 (Fig. 2I–J). The 10 mg/kg dose of ELB00824 also briefly reduced oxaliplatin induced cold hyperalgesia but not mechanical allodynia at 1 h following injection (Fig. 2I–J). The 3 mg/kg dose had no effect on either cold hyperalgesia or mechanical allodynia induced by oxaliplatin.

3.2. The PPARγ antagonist blocks ELB00824 prevention of OIPN

To determine whether ELB00824 specifically targets PPARγ and whether ELB00824 prevents OIPN via a peripheral or central route, we injected a specific PPARγ antagonist T0070907 via i.p. or i.t. injection in OIPN mice treated with ELB00824. We also compared the efficacy of ELB00824 on OIPN prevention with a peripherally restricted PPARγ agonist pioglitazone. Both T0070907 injected via i.p. and i.t significantly blocked the preventative effect of preemptive ELB00824 on OIPN, suggesting that ELB00824 likely acts on both central and peripheral PPARγ to mediate pain prevention in OIPN. Peripherally administered pioglitazone at 30 mg/kg had no effect on OIPN, suggesting pioglitazone is less efficacious in preventing OIPN than ELB00824 via i.p. route in our model (Fig. 3).

3.3. Opposing effect of ELB00824 on oxaliplatin-induced hyperexcitability in IB4− and IB4+ DRG neurons

Next, we examined the direct effect of ELB00824 on oxaliplatin induced DRG neuron excitability using whole-cell current clamp. *In vitro* treatment of DRG neurons for 1 h prior to recording with oxaliplatin (50 μM) induced increased firing in both $IB4^-$ and $IB4^+$ neurons compared to vehicle controls. However, the magnitude of change in firing frequency-induced by oxaliplatin was larger in $IB4^-$ neurons, suggesting that this population is more susceptible to oxaliplatin-induced hyperexcitability. ELB00824 significantly inhibited oxaliplatin-induced firing in $IB4^-$ neurons, but paradoxically increased oxaliplatin-induced firing in $IB4^+$ neurons (Fig. 4).

3.4. ELB00824 reduces oxaliplatin-induced oxidative stress in HEK cells, DRGs, and the spinal cord

Since oxidative stress induced by oxaliplatin is a major contributing factor to the OIPN (Zajączkowska et al., 2019), we first examined the effect of ELB00824 on oxidative stress. In HEK293 cells, we examined dose-response inhibition of ROS H_2O_2 generation and best-fit curves for compounds ELB00824, rosiglitazone, and pioglitazone. The half maximal effective concentration (EC_{50}) and maximal activities (% control) were 1.5 μM and 48% for ELB00824; 2.7 μM and 60% for rosiglitazone; and nhjm0.65 μM and 42% for pioglitazone, respectively (Fig. 5A). Therefore, ELB00824 exhibited *in vitro* anti-oxidative activity in HEK293 cells similar to typical clinically used PPARγ agonists. In the chronic OIPN model, we found that compared with the vehicle control group, chronic oxaliplatin treatment resulted in a significant increase in spinal oxidative stress, evidenced by significant increase of the protein carbonyl (Figure 5B), 3-nitrotyrosine (Fig. 5C) and TBARS levels (Fig. 5D). Preemptive i.p. injections of ELB00824 (30 mg/kg), but not pioglitazone (30 mg/kg), resulted in a significant reduction in spinal carbonyl, 3-nitrotyrosine and TBARS levels. In the acute OIPN model, we measured *Pparg* and genes involved in oxidative stress such as *Sod2*, *Cat*, and *Ppargc1a* in the DRG and the spinal cord. i.p. injections of ELB00824 (30 mg/kg), but not pioglitazone (30 mg/kg), increased gene expression of *Pparg*, *Sod2*, *Cat*, and *Ppargc1a* in the DRG and the spinal cord compared to the mice treated with oxaliplatin alone (Fig. 6).

3.5. CNS safety assessment of ELB00824

To determine whether ELB00824 has any effect on neuromuscular coordination/sedation, we assessed mouse motor performance with a beam-walking test. The positive control Carbamazepine (Carb, 30 mg/kg, i.p.), a marketed analgesic, significantly increased the time to traverse and number of errors (Fig. 7A and B) in mice in the beam-walking test. The impairment of motor performance was only observed in high doses of ELB00824 (90 and 120 mg/kg, i.p.), which significantly increased the time to traverse and number of errors in mice (Fig. 7A and B); but the 10, 30, and 60 mg/kg doses had no effect.

To determine the potential addictive effect of ELB00824, we used the CPP test with two doses, 30 and 60 mg/kg that did not cause any motor incoordination/sedation in the beam-walking test. CPP was reflected as a preference for the drug-paired context, e.g, striped (Fig. 7C) or blank (Fig. 7D) or side of CPP box, with the vehicle control group showing

no preference for either context. The positive control morphine (5 mg/kg) significantly increased the post-conditioning time spent in morphine-paired context. In contrast, no significant difference between the pre-conditioning and post-conditioning times was found in mice for the ELB00824-paired context (Fig. 7C and D), indicating that ELB00824 did not induce a preference or an aversion for the drug-paired compartment at a dose as high as 60 mg/kg. Therefore, the maximal tolerated dose (MTD) for ELB00824 is approximately 60 mg/kg.

3.6. ELB00824 did not affect anti-cancer effect of oxaliplatin in vitro

To address whether ELB00824 interferes the anti-cancer effect of oxaliplatin, we conducted MTS-based proliferation assays using two different human cancer cell lines (a colorectal carcinoma line HCT116 and an oral squamous carcinoma cell line HSC-3). Graded concentrations of ELB00824 did not inhibit the proliferation of these human cancer cell lines, while oxaliplatin inhibited colon and oral cancer cell proliferation in a concentration-dependent manner. ELB00824 (10, or 30 μM) added together with oxaliplatin in these two cancer cell lines, did not change the 50% inhibitory concentration (IC_{50}) of oxaliplatin on proliferation (Fig. 8). These results indicate that ELB00824 did not alter the anti-cancer effect of oxaliplatin.

4. Discussion

PPARγ agonists are becoming a promising pharmacological strategy for CIPN, inspired by several animal studies where diabetic compounds such as rosiglitazone and pioglitazone exhibited protection against cellular oxidative stress and mitochondrial damage (Zanardelli et al., 2014; Khasabova et al., 2019), interfered the synthesis of important pain mediators, as well as suppressed cancer progression (Quintão et al., 2019). Additionally, two clinical trials reported that palmitoylethanolamide, a naturally occurring PPARγ agonist (Paterniti et al., 2013), provided significant restoration of myelinated afferent nerve function, possibly by protection against spinal glia-activation and moderating mast cell hyperactivity in CIPN (Truini et al., 2011; Zaiss et al., 2021). However, not all animal studies demonstrate a beneficial effect of PPARγ agonists against CIPN (Jain et al., 2011), and in clinical studies with large sample size, no PPARγ agonists have been proven to be neuroprotective (Brundin and Wyse, 2015). In the present study, we tested safety and efficacy of a new PPARγ agonist, ELB00824, with good BBB permeability, in acute and chronic OIPN mouse models. We found that ELB00824 exerts both preventative as well as acute treatment effect on OIPN, via both peripheral and central mechanisms. ELB00824 is safe, with an improved therapeutic window, and is more efficacies in preventing OIPN and oxidative stress than other PPARγ agonists with low BBB permeability.

4.1. Therapeutic window and BBB permeability of ELB00824

Lack of therapeutic window is one of the major issues of many pain relief therapies used today, e.g., cannabis (Hill et al., 2017). Therapeutic window is determined as a range between the minimum effective dose (MED) and the maximum tolerated dose (MTD). Here the mouse chronic model of OIPN was used to analyze the preventive therapeutic window of ELB00824. The human oral MTD for pioglitazone was reported to be 45 mg per day with

bioavailability at 83%, equivalent to 11 mg/kg (i.p.) for mouse MTD (Nair and Jacob, 2016), which is much lower than mouse i.p. MED (>30 mg/kg, if any) as determined in the present study (Fig. 3). Therefore, no therapeutic window exists for pioglitazone in the chronic OIPN model. In contrast, the mouse i.p. MED of ELB00824 is 10 mg/kg for OIPN (Fig. 2E and F). In the motor performance assay, the mouse i.p. MTD is determined to be 60 mg/kg, thus the therapeutic window relative to motor coordination/sedation is 6-fold (MTD/MED = 60/10 = 6). Regarding abuse and addiction potential, ELB00824 did not induce a preference or an aversion for the drug-paired compartment at the dose up to 60 mg/kg, indicating the therapeutic window relative to addiction is at least 6-fold (MTD/MED = 60/10 = 6). In comparison, morphine (a positive control) induced a preference at the dose as low as 5 mg/kg. These toxicological data suggested that ELB00824 is safe upon CNS entry, and the therapeutic window relative to CNS side effect is 6-fold or higher, while pioglitazone has no therapeutic window as demonstrated by our data.

The improved efficacy of ELB00824 on OIPN compared to pioglitazone could be due to its higher BBB permeability. The BBB permeability (indicated by log BB value) of pioglitazone after i.p. injection at 10 mg/kg was reported to be very poor, and accordingly, BBB limits the peak CNS concentration to the range of 1 μM (Chang et al., 2015; Zhang et al., 2019; Westlund and Zhang,2020). In fact, the log BB value of almost all the current PPARγ agonists, e.g., rosiglitazone (−0.727), pioglitazone (−0.561), or palmitoylethanolamine (−0.441) was calculated to be unacceptably low, calculated by pkCSM, a web server predicting small-molecule pharmacokinetic properties (Pires et al., 2015; Westlund and Zhang, 2020). The log BB values (i.e., the ratio of the concentration in the brain and in the blood) using of current PPARγ agonists are much less (difference >1.0) than that of ELB00824 (0.747), indicating their concentration in CNS is at least one order in magnitude lower than ELB00824. Our previous study further indicated the activity of pioglitazone in CNS was negligible relative to ELB00824 (Zhang et al., 2019). When injected i.p. into rats with the dose of 10 mg/kg, the brain peak concentration of pioglitazone is 1.7 μM, which is only 8% (1.7 μM/22 μM × 100%) of the *in vitro* EC_{50} (22 μM) for PPARγ activation. In contrast, the brain peak concentration of ELB00824 is 9.4 μM, which is as high as 145% (9.4 μM/6.5 μM × 100%) of the *in vitro* EC_{50} (6.5 μM) for PPARγ activation.

4.2. ELB00824 inhibited oxaliplatin-induced neuronal hypersensitivity in IB4⁻ neurons

At the peripheral level, ELB00824 inhibited oxaliplatin-induced neuronal hypersensitivity in $IB4^-$ neurons, but paradoxically increased oxaliplatin-induced neuronal hypersensitivity in $IB4^+$ neurons. Recently, it has been shown that oxaliplatin selectively increased the membrane excitability of the $IB4^-$, but not the $IB4^+$ small DRG neurons (Wu et al., 2021), indicating that $IB4^-$ DRG neurons are the major contributor of OIPN. These findings are supported by other studies showing that oxaliplatin treatment upregulates several members of the TRP channels (e.g., TPRA1, TRPM8, and TRPV1) preferentially expressed in $IB4^-$ DRG neurons, and antagonism or gene deficiency of these channels abolishes CIPN (Descoeur et al., 2011). However, we cannot completely rule out the contribution of $IB4^+$ neurons to OIPN, as ablation of $IB4^+$ neurons using neuronal toxin saporin has been shown to reduce OIPN in rats (Joseph et al., 2008). In our study, oxaliplatin induced increased

firing in both $IB4^+$ and $IB4^-$ neurons, with a statistically more significant effect on $IB4^-$ neurons. It is unknown why ELB00824 increased oxaliplatin-induced neuronal firing in $IB4^+$ neurons; however, this observation does not nullify the beneficial effect of ELB00824. The nociceptive output is a balance act between the excitatory and inhibitory input. Based on our data, the inhibitory effect of ELB00824 surpasses the excitatory effect, which suggest an overall inhibitory effect of ELB00824 on peripheral neuronal hypersensitivity induced by oxaliplatin.

The electrophysiological data support a fast action of ELB00824 on sensory neurons as the recordings are performed following acute treatment of ELB00824. In our behavioral assays, we also observed a rapid analgesic effect induced by ELB00824, similar to others who also reported a rapid anti-nociceptive effect exerted by PPARγ agonists (Griggs et al., 2016; Churi et al., 2008; Donvito et al., 2016). These data are consistent with transcription-independent function of PPARγ, in addition to its transcription-dependent function. The reported transcription independent roles of PPARγ include modified protein-protein interaction induced by conformation changes of PPARγ upon the binding of agonists (Trümper et al., 2020), activation or inhibition of kinases and phosphatases (Luconi et al., 2010; Griggs et al., 2016; Maruta et al., 2019), or modulation of a variety of ion channel activities such as sodium, potassium, calcium, and TRP channels (Hung et al., 2019; Omae et al., 2011; Gu et al., 2014; Heppner et al., 2005; Majeed et al., 2011).

4.3. ELB00824 reduced oxaliplatin induced oxidative stress

Oxidative stress is a well-known mechanism underlying CIPN, and oxaliplatin has been shown to induce increased oxidative stress (e.g., carbonylated protein and TBARS) in the rat spinal cord (Zanardelli et al., 2014) and brain (Waseem and Parvez, 2016). PPARγ transcriptionally upregulate several enzymes, including Sod2, Cat, Ppargc1a, which are very important for oxidative stress, mitochondrial biogenesis and function (Khasabova et al., 2019; Portilla et al., 2002). PPARγ agonists alone can lead to upregulation of these key antioxidant enzymes in the CNS (Yu et al., 2008). Platinum based chemotherapies have been shown to reduce the expression and activity of PPARγ as well as these enzymes involved in oxidative stress in different types of neuronal tissues (Janes et al., 2013; Areti et al., 2017; Khasabova et al., 2019; Waseem and Parvez, 2016; Zanardelli et al., 2014), while cotreatment with PPARγ agonists (e.g., pioglitazone) blocked all these effects. Our data are consistent with known effect of oxaliplatin on oxidative stress and support the hypothesis that PPARγ activation prevents oxaliplatin-induced oxidative stress, and consequentially may preserve mitochondria bioenergetics and reduces OIPN.

To our surprise, in both our acute and chronic models of OIPN, we found that ELB00824 but not pioglitazone, i.p. administered at the same dose, reduced oxaliplatin induced oxidative stress. While ELB00824 may induce higher spinal PPARγ activity due to its much higher BBB permeability, which results in an increased reduction of spinal oxidative stress, it is unknown why pioglitazone had no effect on *Pparg*, *Sod2*, *Cat*, and *Ppargc1a* gene expression in the DRG. In HEK cells, the anti-oxidative activities are comparable between ELB00824 and pioglitazone based on IC_{50}. It is likely that the anti-oxidative activities of ELB00824 and pioglitazone are tissue-dependent.

4.4. Comparison with other PPARγ agonists in OIPN

To date, only a few papers have studied the preclinical effects of PPARγ agonists in OIPN. Among them, one paper claimed non-beneficial effects of low BBB permeable PPARγ agonists (i.e., rosiglitazone) in oxaliplatin-mediated oxidative stress or CIPN (Jain et al., 2011), which is in agreement with our data. On the other hand, 5 papers showed that their low BBB permeable PPARγ agonists (i.e., rosiglitazone, tesaglitazar, pioglitazone, palmitoylethanolamine and new TZDs) reduced CIPN in Sprague-Dawley rats (2.4 mg/kg, i.p. for 5 consecutive days every week for 3 weeks, equivalent to a total HED of 1332 mg/m^2)(Zanardelli et al., 2014; Di Cesare Mannelli et al., 2015), Wistar rats (2 mg/kg, i.p. for 5 consecutive days with cumulative dosages of 10 mg/kg, equivalent to a total HED of 370 mg/m^2) (Nair and Jacob, 2016; Campolo et al., 2021), or in C57BL/6 mouse models (3 mg/kg, single i.p. equivalent to a HED of 111 mg/m^2)(Moreira et al., 2017). One of these papers also demonstrated that pioglitazone prevented spinal oxidative alterations by reducing lipid peroxidation and carbonylated protein levels in Sprague-Dawley rats (2.4 mg/kg, i.p. for 5 consecutive days every week for 3 weeks, Zanardelli et al., 2014). The controversy between ours and other studies may be explained by differences in the treatment route, dose and duration, animal strain and species used. First, all these studies used the intraperitoneal whereas we used the intravenous administration of oxaliplatin. The intravenous route is the most frequently used for neurotoxic antineoplastic drugs including oxaliplatin; at the same drug dose, the i.v. administration route has a much higher systemic drug exposure than the i.p. route (Pozzi et al., 2020). Second, other studies used a lower accumulative HED and shorter treatment schedule of oxaliplatin than our chronic model (i.e., 1480 mg/m2 for 4 weeks); nevertheless, an accumulative oxaliplatin HED higher than 540 mg/m^2 is usually required for patients to develop chronic neuropathies (Extra et al., 1998). Third, it has been reported that, compared to C57BL/6 and other mouse strains, our BALB/c mice are more severely affected by oxaliplatin (Marmiroli et al., 2017; Warncke et al., 2021). Consistent with this, oxaliplatin treatment induces neuronal hypersensitivities in both IB4$^+$ and IB4$^-$ neurons in our BALB/c mice, but selectively affect IB4$^-$ neurons in C57BL/6 mice (Wu et al., 2021). These abovementioned differences provide a rationale for why low BBB permeable PPARγ agonists reduced CIPN and prevented spinal oxidative alterations in other rodent models, but not in our models. However, we cannot exclude other differences in experimental methods, which may impact the results.

4.5. Limitations

Our study has several limitations. First, we only tested the impact of ELB00824 on the anti-neoplastic effect of oxaliplatin *in vitro;* a non-tumor bearing CIPN *in vivo* model is used. Although non-tumor bearing CIPN models are widely used, which allow us to compare our results with others, using a tumor-bearing model of CIPN and simultaneously examining the effect of repeated preemptive ELB00824 injection on OIPN and tumor progression will be a closer resemblance of cancer patients under chemotherapy. Second, PPARγ agonists are known to influence other mechanisms important to CIPN (reviewed in Quintão et al., 2019), such as ion channel dysfunction and neuroinflammation; the present study only focused on oxidative stress. Additional studies are underway to address other downstream mechanisms ELB00824 may be involved in, and why ELB00824 exerts opposing effect in IB4$^+$ and IB4$^-$ neurons subjected to oxaliplatin treatment.

5. Conclusion

In the present study, we examined the efficacy and safety of a highly BBB permeable PPARγ agonist ELB00824 in mouse models of OIPN. Our data showed that ELB00824 was more efficacious than low BBB permeable PPARγ agonist pioglitazone in reducing OIPN (*i.e.*, cold hyperalgesia and mechanical allodynia) and oxidative stress. ELB00824 suppressed oxaliplatin-induced neuronal hypersensitivities in $IB4^{-}$ neurons. ELB00824 exhibited a good therapeutic window tolerating neurological side effects (*i.e.*, motor incoordination/sedation and abuse liability) and did not influence the anti-neoplastic effect of oxaliplatin *in vitro*. Therefore, we conclude that ELB00824 potentially could serve as an attractive drug candidate to mitigate CIPN.

Acknowledgements

This work was supported in part by the National Institutes of Health [R21 DE028096 (KNW), 1UG3NS123958-01 (KNW, SRAA), NIH R01 DE029493 (YY)], Department of Defense W81XWH-20-1-0930 (KNW and SRAA) and the Research Endowment fund of the Dept of Anesthesiology and Critical Care Medicine, UNM HSC (KNW and SRAA), and the private funding from USA Elixiria Biotech Inc. (MZ)

Data availability

Data will be made available on request.

Abbreviations

ATCC	American Type Culture Collection
BBB	Blood-Brain Barrier
CAT	Catalase
CPP	Conditioned Place Preference
CIPN	Chemotherapy-Induced Peripheral Neuropathy
CNS	Central Nervous System
DPI	Days post-initiation of treatment with chemicals or vehicles
DRG	Dorsal Root Ganglion
ELB	ELB00824
GW	GW9662
HED	Human Equivalent Dose
IB4	Isolectin B4
i.p.	Intraperitoneal
i.v.	Intravenous
i.t.	Intrathecal

MED	Minimum Effective Dose
MEK	Mitogen-activated protein kinase kinase
MnSOD	Manganese Superoxide Dismutase
MTD	Maximum Tolerated Dose
OIPN	Oxaliplatin-Induced Peripheral Neuropathy
Oxa	Oxaliplatin
PCO	Protein Carbonyls
PGC-1α	Peroxisome proliferator–activated receptor gamma coactivator-1 alpha
PKC	Protein kinase C
PNS	Peripheral Nervous System
Pio	Pioglitazone
ROS	Reactive Oxygen Species
SEM	Standard error of the mean
SD	Standard deviation
SOD2	Superoxide dismutase 2
T00	T0070907
TBARS	Thiobarbituric acid reactive substances
TZD	Thiazolidinedione
Veh	Vehicle

References

Alsalem M, Haddad M, Aldossary SA, Kalbouneh H, Azab B, Dweik A, Imraish A, El-Salem K.l., 2019. Effects of dual peroxisome proliferator-activated receptors α and γ activation in two rat models of neuropathic pain. PPAR Res. 2019, 2630232. [PubMed: 31139213]

Areti A, Komirishetty P, Akuthota M, Malik RA, Kumar A, 2017. Melatonin prevents mitochondrial dysfunction and promotes neuroprotection by inducing autophagy during oxaliplatin-evoked peripheral neuropathy. J. Pineal Res. 62.

Boland EG, Selvarajah D, Hunter M, 2014. Central pain processing in chronic chemotherapy-induced peripheral neuropathy: a functional magnetic resonance imaging study. PLoS One 9, e96474. [PubMed: 24821182]

Brenner DS, Golden JP, Gereau RW, 2012. A novel behavioral assay for measuring cold sensation in mice. PLoS One 7, e39765. [PubMed: 22745825]

Brundin P, Wyse R, 2015. Parkinson disease: laying the foundations for diseasemodifying therapies in PD. Nat. Rev. Neurol. 11, 553–555. [PubMed: 26303855]

Campolo M, Lanza M, Paterniti I, Filippone A, Ardizzone A, Casili G, Scuderi SA, Puglisi C, Mare M, Memeo L, Cuzzocrea S, Esposito E, 2021. PEA-OXA mitigates oxaliplatin-induced painful neuropathy through NF-κB/Nrf-2 Axis. Int. J. Mol. Sci. 22, 3927. [PubMed: 33920318]

Chang KL, Pee HN, Yang S, Ho PC, 2015. Influence of drug transporters and stereoselectivity on the brain penetration of pioglitazone as a potential medicine against Alzheimer's disease. Sci. Rep. 5, 9000. [PubMed: 25760794]

Chaplan SR, Bach FW, Pogrel JW, Chung JM, Yaksh TL, 1994. Quantitative assessment of tactile allodynia in the rat paw. J. Neurosci. Methods 53, 55–63. [PubMed: 7990513]

Colombo G, Clerici M, Garavaglia ME, Giustarini D, Rossi R, Milzani A, Dalle-Donne I, 2016. A step-by-step protocol for assaying protein carbonylation in biological samples. J. Chromatogr., B: Anal. Technol. Biomed. Life Sci. 1019, 178–190.

Churi SB, Abdel-Aleem OS, Tumber KK, Scuderi-Porter H, Taylor BK, 2008. Intrathecal rosiglitazone acts at peroxisome proliferatoractivated receptor-gamma to rapidly inhibit neuropathic pain in rats. J. Pain 9, 639–649. [PubMed: 18387855]

Descoeur J, Pereira V, Pizzoccaro A, Francois A, Ling B, Maffre V, Couette B, Busserolles J, Courteix C, Noel J, Lazdunski M, Eschalier A, Authier N, Bourinet E, 2011. Oxaliplatin-induced cold hypersensitivity is due to remodelling of ion channel expression in nociceptors. EMBO Mol. Med. 3, 266–278. [PubMed: 21438154]

Di Cesare Mannelli L, Pacini A, Corti F, Boccella S, Luongo L, Esposito E, Cuzzocrea S, Maione S, Calignano A, Ghelardini C, 2015. Antineuropathic profile of N-palmitoylethanolamine in a rat model of oxaliplatin-induced neurotoxicity. PLoS One 10, e0128080. [PubMed: 26039098]

Donvito G, Wilkerson JL, Damaj MI, Lichtman AH, 2016. Palmitoylethanolamide reverses paclitaxel-induced allodynia in mice. J. Pharmacol. Exp. Therapeut. 359, 310–318.

Fang X, Djouhri L, McMullan S, Berry C, Waxman SG, Okuse K, Lawson SN, 2006. Intense isolectin-B4 binding in rat dorsal root ganglion neurons distinguishes C-fiber nociceptors with broad action potentials and high Nav1.9 expression. J. Neurosci. 26, 7281–7292. [PubMed: 16822986]

G KK, Thaggikuppe Krishnamurthy P, Ammu VVVRK, Vishwanath K, Narenderan ST, Babu B, Krishnaveni N, 2021. Development and validation of a sensitive LC-MS/MS method for pioglitazone: application towards pharmacokinetic and tissue distribution study in rats. RSC Adv. 11, 11437–11443. [PubMed: 35423625]

Goins AE, Gomez K, Ran D, Afaghpour-Becklund M, Khanna R, Alles SRA, 2022. Neuronal allodynic mechanisms of Slc7a5 (LAT1) in the spared nerve injury rodent model of neuropathic pain. Pflügers Archiv 474, 397–403. [PubMed: 35048187]

Griggs RB, Donahue RR, Adkins BG, Anderson KL, Thibault O, Taylor BK, 2016. Pioglitazone inhibits the development of hyperalgesia and sensitization of spinal nociresponsive neurons in type 2 diabetes. J. Pain 17, 359–373. [PubMed: 26687453]

Gu J, Hu W, Liu X, 2014. Pioglitazone improves potassium channel remodeling induced by angiotensin II in atrial myocytes. Med. Sci. Monit. Basic Res. 20, 153–160. [PubMed: 25296378]

Heppner TJ, Bonev AD, Eckman DM, Gomez MF, Petkov GV, Nelson MT, 2005. Novel PPARgamma agonists GI 262570, GW 7845, GW 1929, and pioglitazone decrease calcium channel function and myogenic tone in rat mesenteric arteries. Pharmacology 73, 15–22. [PubMed: 15452359]

Hill KP, Palastro MD, Johnson B, Ditre JW, 2017. Cannabis and pain: a clinical review. Cannabis Cannabinoid Res 2, 96–104. [PubMed: 28861509]

Hu LY, Mi WL, Wu GC, Wang YQ, Mao-Ying QL, 2019. Prevention and treatment for chemotherapy-induced peripheral neuropathy: therapies based on CIPN mechanisms. Curr. Neuropharmacol. 17, 184–196. [PubMed: 28925884]

Hung TY, Chu FL, Wu DC, Wu SN, Huang CW, 2019. The protective role of peroxisome proliferator-activated receptor-gamma in seizure and neuronal excitotoxicity. Mol. Neurobiol. 56, 5497–5506. [PubMed: 30623373]

Huang ZZ, Li D, Ou-Yang HD, Liu CC, Liu XG, Ma C, Wei JY, Liu Y, Xin WJ, 2016. Cerebrospinal fluid oxaliplatin contributes to the acute pain induced by systemic administration of oxaliplatin. Anesthesiology 124, 1109–1121. [PubMed: 26978408]

Jain V, Jaggi AS, Singh N, 2011. Non-beneficial effects of rosiglitazone in oxaliplatin-induced cold hyperalgesia in rats. J. Pharm. Negat. Results 2, 28–34.

Janes K, Doyle T, Bryant L, Esposito E, Cuzzocrea S, Ryerse J, Bennett GJ, Salvemini D, 2013. Bioenergetic deficits in peripheral nerve sensory axons during chemotherapyinduced neuropathic pain resulting from peroxynitrite-mediated post-translational nitration of mitochondrial superoxide dismutase. Pain 154, 2432–2440. [PubMed: 23891899]

Joseph EK, Chen X, Bogen O, Levine JD, 2008. Oxaliplatin acts on IB4-positive nociceptors to induce an oxidative stress-dependent acute painful peripheral neuropathy. J. Pain 9, 463–472. [PubMed: 18359667]

Khasabova IA, Khasabov SG, Olson JK, Uhelski ML, Kim AH, Albino-Ramírez AM, Wagner CL, Seybold VS, Simone DA, 2019. Pioglitazone, a PPARγ agonist, reduces cisplatin-evoked neuropathic pain by protecting against oxidative stress. Pain 160, 688–701. [PubMed: 30507781]

Li Y, Adamek P, Zhang H, Tatsui CE, Rhines LD, Mrozkova P, Li Q, Kosturakis AK, Cassidy RM, Harrison DS, Cata JP, Sapire K, Zhang H, Kennamer-Chapman RM, Jawad AB, Ghetti A, Yan J, Palecek J, Dougherty PM, 2015. The cancer chemotherapeutic paclitaxel increases human and rodent sensory neuron responses to TRPV1 by activation of TLR4. J. Neurosci. 35, 13487–13500. [PubMed: 26424893]

Luconi M, Cantini G, Serio M, 2010. Peroxisome proliferator-activated receptor gamma (PPARgamma): is the genomic activity the only answer? Steroids 75, 585–594. [PubMed: 19900469]

Lyons DN, Zhang L, Danaher RJ, Miller CS, Westlund KN, 2017. PPARγ agonists attenuate trigeminal neuropathic pain. Clin. J. Pain 33, 1071–1080. [PubMed: 28514232]

Ma J, Kavelaars A, Dougherty PM, Heijnen CJ, 2018. Beyond symptomatic relief for chemotherapy-induced peripheral neuropathy: targeting the source. Cancer 124, 2289–2298. [PubMed: 29461625]

Majeed Y, Bahnasi Y, Seymour VA, Wilson LA, Milligan CJ, Agarwal AK, Sukumar P, Naylor J, Beech DJ, 2011. Rapid and contrasting effects of rosiglitazone on transient receptor potential TRPM3 and TRPC5 channels. Mol. Pharmacol. 79, 1023–1030. [PubMed: 21406603]

Maldonado R, Saiardi A, Valverde O, Samad TA, Roques BP, Borrelli E, 1997. Absence of opiate rewarding effects in mice lacking dopamine D2 receptors. Nature 388, 586–589. [PubMed: 9252189]

Marmiroli P, Riva B, Pozzi E, Ballarini E, Lim D, Chiorazzi A, Meregalli C, Distasi C, Renn CL, Semperboni S, Morosi L, Ruffinatti FA, Zucchetti M, Dorsey SG, Cavaletti G, Genazzani A, Carozzi VA, 2017. Susceptibility of different mouse strains to oxaliplatin peripheral neurotoxicity: phenotypic and genotypic insights. PLoS One 12, e0186250. [PubMed: 29020118]

Maruta T, Nemoto T, Hidaka K, Koshida T, Shirasaka T, Yanagita T, Takeya R, Tsuneyoshi I, 2019. Upregulation of ERK phosphorylation in rat dorsal root ganglion neurons contributes to oxaliplatin-induced chronic neuropathic pain. PLoS One 14, e0225586. [PubMed: 31765435]

Moreira DRM, Santos DS, Espírito Santo RFD, Santos FED, de Oliveira Filho GB, Leite ACL, Soares MBP, Villarreal CF, 2017. Structural improvement of new thiazolidinones compounds with antinociceptive activity in experimental chemotherapy-induced painfμl neuropathy. Chem. Biol. Drug Des. 90, 297–307. [PubMed: 28112878]

Nair AB, Jacob S, 2016. A simple practice guide for dose conversion between animals and human. J. Basic Clin. Pharm. 7, 27–31. [PubMed: 27057123]

Noh MC, Stemkowski PL, Smith PA, 2019. Long-term actions of interleukin-1β on K+, Na+ and Ca2+ channel currents in small, IB4-positive dorsal root ganglion neurons; possible relevance to the etiology of neuropathic pain. J. Neuroimmunol. 332, 198–211. [PubMed: 31077855]

Okhawa H, Ohishi N, Yagi K, 1979. Assay for lipid peroxidation in animal tissue by thiobarbituric acid reaction. Anal. Biochem. 95, 351–358. [PubMed: 36810]

Omae T, Nagaoka T, Tanano I, Yoshida A, 2011. Pioglitazone, a peroxisome proliferator-activated receptor-γ agonist, induces dilation of isolated porcine retinal arterioles: role of nitric oxide and potassium channels. Invest. Ophthalmol. Vis. Sci. 52, 6749–6756. [PubMed: 21757589]

Paterniti I, Impellizzeri D, Crupi R, Morabito R, Campolo M, Esposito E, Cuzzocrea S, 2013. Molecular evidence for the involvement of PPAR-δ and PPAR-γ in anti-inflammatory and neuroprotective activities of palmitoylethanolamide after spinal cord trauma. J. Neuroinflammation 10, 20. [PubMed: 23374874]

Portilla D, Dai G, McClure T, Bates L, Kurten R, Megyesi J, Price P, Li S, 2002. Alterations of PPARalpha and its coactivator PGC-1 in cisplatin-induced acute renal failure. Kidney Int. 62, 1208–1218. [PubMed: 12234291]

Pozzi E, Fumagalli G, Chiorazzi A, Canta A, Meregalli C, Monza L, Carozzi VA, Oggioni N, Rodriguez-Menendez V, Cavaletti G, Marmiroli P, 2020. The relevance of multimodal assessment in experimental oxaliplatin-induced peripheral neurotoxicity. Exp. Neurol. 334, 113458. [PubMed: 32889007]

Pires DE, Blundell TL, Ascher DB, 2015. pkCSM: predicting small-molecule pharmacokinetic properties using graph-based signatures. J. Med. Chem. 58, 4066–4072. [PubMed: 25860834]

Quintão NLM, Santin JR, Stoeberl LC, Corrêa TP, Melato J, Costa R, 2019. Pharmacological treatment of chemotherapy-induced neuropathic pain: PPARγ agonists as a promising tool. Front. Neurosci. 13, 907. [PubMed: 31555078]

Stucky CL, Lewin GR, 1999. Isolectin B4-positive and -negative nociceptors are functionally distinct. J. Neurosci. 19, 6497–6505. [PubMed: 10414978]

Truini A, Biasiotta A, Di Stefano G, La Cesa S, Leone C, Cartoni C, Federico V, Petrucci MT, Cruccu G, 2011. Palmitoylethanolamide restores myelinated-fibre function in patients with chemotherapy-induced painful neuropathy. CNS Neurol. Disord.: Drug Targets 10, 916–920.

Trümper V, Wittig I, Heidler J, Richter F, Brüne B, von Knethen A, 2020. Redox regulation of PPARγ in polarized macrophages. PPAR Res. 2020, 8253831. [PubMed: 32695149]

Warncke UO, Toma W, Meade JA, Park AJ, Thompson DC, Caillaud M, Bigbee JW, Bryant CD, Damaj MI, 2021. Impact of dose, sex, and strain on oxaliplatin-induced peripheral neuropathy in mice. Front Pain Res. (Lausanne) 2, 683168. [PubMed: 35295533]

Waseem M, Parvez S, 2016. Neuroprotective activities of curcumin and quercetin with potential relevance to mitochondrial dysfunction induced by oxaliplatin. Protoplasma 253, 417–430. [PubMed: 26022087]

Westlund KN, Zhang M, 2020. Building and testing PPARγ therapeutic ELB00824 with an improved therapeutic window for neuropathic pain. Molecules 25, 1120.

Wu B, Su X, Zhang W, Zhang YH, Feng X, Ji YH, Tan ZY, 2021. Oxaliplatin depolarizes the IB4− dorsal root ganglion neurons to drive the development of neuropathic pain through TRPM8 in mice. Front. Mol. Neurosci. 14, 690858. [PubMed: 34149356]

Yu X, Shao XG, Sun H, Li YN, Yang J, Deng YC, Huang YG, 2008. Activation of cerebral peroxisome proliferator-activated receptors gamma exerts neuroprotection by inhibiting oxidative stress following pilocarpine-induced status epilepticus. Brain Res. 1200, 146–158. [PubMed: 18289512]

Zaiss M, Uhlig J, Zahn MO, Decker T, Lehmann HC, Harde J, Hogrefe C, Vannier C, Marschner N, 2021. Improving chemotherapy-induced peripheral neuropathy in patients with breast or colon cancer after end of (Neo)adjuvant therapy: results from the observational study STEFANO. Oncol. Res. Treat. 44, 613–621. [PubMed: 34496363]

Zajączkowska R, Kocot-Kępska M, Leppert W, Wrzosek A, Mika J, Wordliczek J, 2019. Mechanisms of chemotherapy-induced peripheral neuropathy. Int. J. Mol. Sci. 20, 1451.

Zanardelli M, Micheli L, Cinci L, Failli P, Ghelardini C, Di Cesare Mannelli L, 2014. Oxaliplatin neurotoxicity involves peroxisome alterations. PPARγ agonism as preventive pharmacological approach. PLoS One 9, e102758. [PubMed: 25036594]

Zhang M, Hu M, Montera MA, Westlund KN, 2019. Sustained relief of trigeminal neuropathic pain by a blood-brain barrier penetrable PPAR gamma agonist. Mol. Pain 15, 1744806919884498. [PubMed: 31588847]

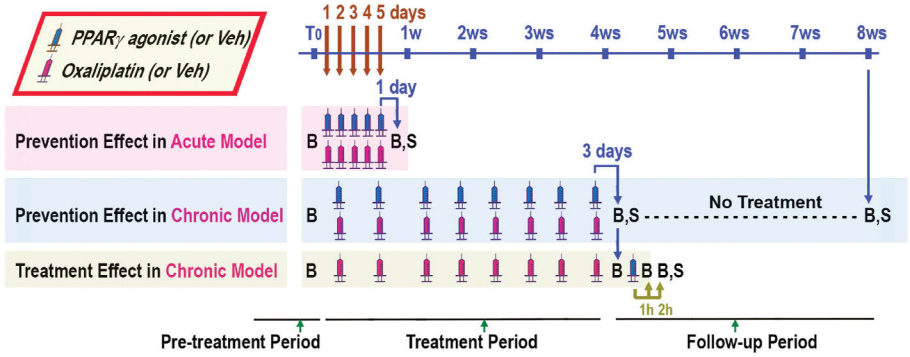

Fig. 1. Flow-chart and timeline of acute and chronic models of OIPN.

In the acute model of OIPN, the oxaliplatin was administrated i.p. once per day for 5 consecutive days; the pain-like behavior tests were carried out on the 1st day after the last dosing. In the chronic model of OIPN, the oxaliplatin was administrated i.v. twice per week for 4 weeks, followed by 4 weeks without any treatment of oxaliplatin; the pain-like behaviors were studied on the 3rd day after the last dosing (at the end of the treatment period), and 4 weeks after the last dosing (at the end of the follow-up period). The timing of PPARγ agonists (ELB00824 or pioglitazone) or their vehicle (Veh) administration is indicated as blue syringes. The timing of oxaliplatin or vehicle (Veh) administration is indicated as red syringes. The prevention effects of ELB00824 were tested by co-administration ELB00824 with oxaliplatin via i.p. The treatment effect of ELB00824 was also tested at pre-dosing, 1 h and 2 h post i.p. dosing of ELB00824 on the 3rd day after the last dosing of oxaliplatin in the chronic model. B: behavior tests. S: Sacrifice and organ collection. T_0: pre-treatment period. h: hour. (For interpretation of the references to colour in this figure legend, the reader is referred to the web version of this article.)

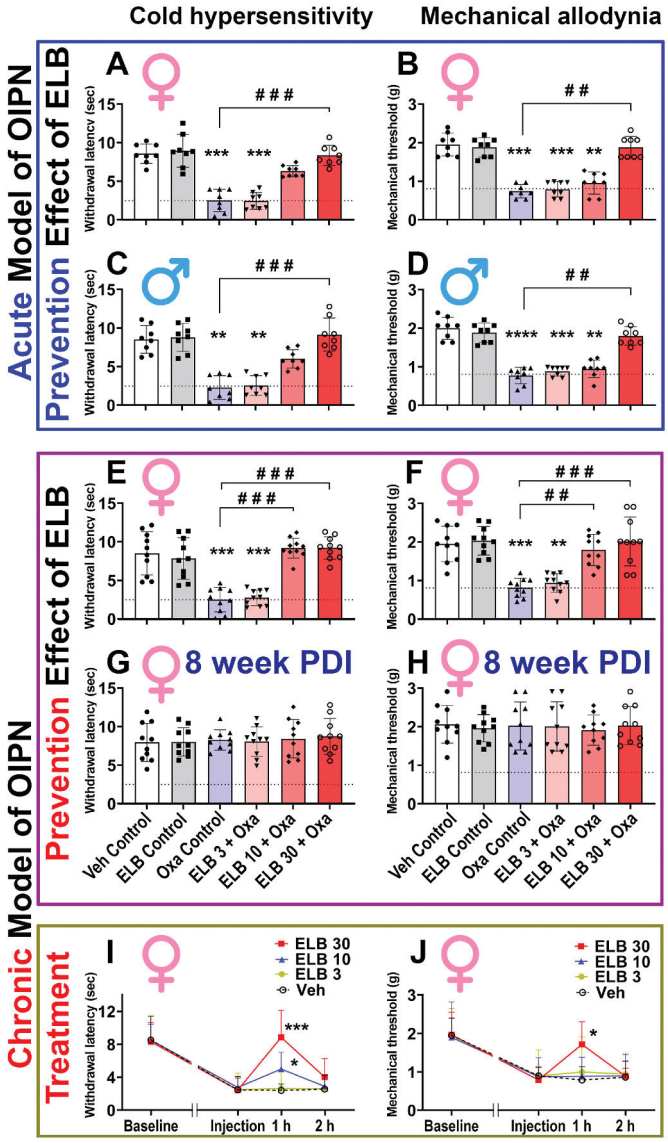

Fig. 2. ELB00824 attenuated cold hyperalgesia and mechanical allodynia produced by oxaliplatin.

(A-D) In the female (A, B) and male (C, D) mouse model of acute OIPN, at the end of oxaliplatin (Oxa) treatment period at day 6 post drug injection (PDI), the prevention effect of ELB00824 (ELB) on cold hyperalgesia (A, C) and mechanical allodynia (B, D) was assessed (n = 8/group). (E-H) In the female mouse model of chronic OIPN, at the end of oxaliplatin treatment period (E, F at 4 week PDI), and follow-up period (G, H at 8 week PDI), the prevention effect of ELB on cold hyperalgesia (E, G) and mechanical allodynia (F, H) was assessed (n = 10/group). (I-J) In the female mouse model of chronic OIPN, at the end of oxaliplatin treatment period, the treatment effect of ELB on cold hyperalgesia (I) and mechanical allodynia (J) was assessed (n = 8/group). ELB 30: ELB00824 30 mg/kg. ELB 10: ELB00824 10 mg/kg. ELB 3: ELB00824 3 mg/kg. Veh: Vehicle. In figures A-H, the box-and-whiskers plots show minimum, maximum, median and 25th and 75th percentiles; while in figure I-J, symbols at mean and error bars at standard deviation (SD)

are superimposed with connecting line. Inter-group comparison was done using one-way ANOVA, followed by Dunn's test. *: $p \leq 0.05$; **: $p \leq 0.01$; ***: $p \leq 0.001$ vs Veh Control or Veh group. #: $p \leq 0.05$; ##: $p \leq 0.01$; ###: $p \leq 0.001$; ####: $p \leq 0.0001$ vs Oxa Control group. Dashed line is the mean value of Oxa control group at the end of oxaliplatin treatment period in the chronic OIPN model.

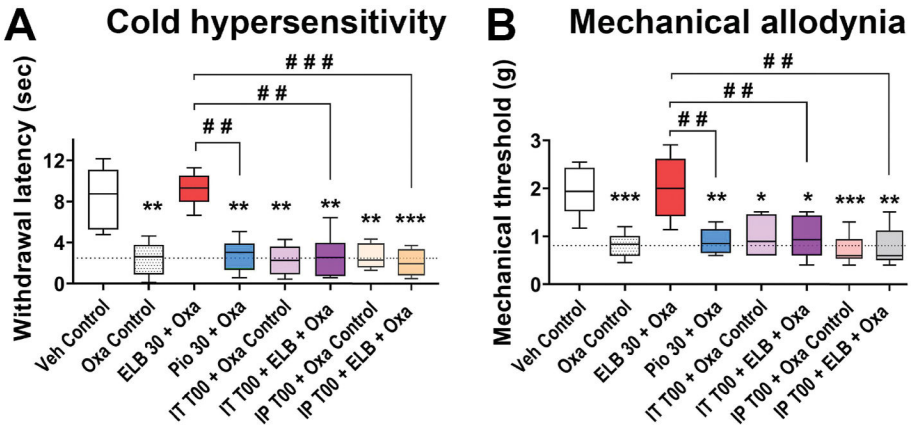

Fig. 3. The PPARγ antagonist blocks ELB00824 prevention of OIPN.

The involvement of PPARγ in the preventive effect of ELB00824 (ELB) on cold hyperalgesia (A) and mechanical allodynia (B) was identified at the end of oxaliplatin treatment period in the chronic model of OIPN. The box-and-whiskers plots show minimum, maximum, median and 25th and 75th percentiles. Inter-group comparison was done using one-way ANOVA, followed by Dunn's test. *: $p \leq 0.05$; **: $p \leq 0.01$; ***: $p \leq 0.001$; ****: $p \leq 0.01$; vs Veh Control group. #: $p \leq 0.05$; ##: $p \leq 0.01$; ###: $p \leq 0.001$ vs ELB 30 + Oxa group. Dashed line is the mean value of Oxa control group at the end of the oxaliplatin treatment period in the chronic OIPN model.

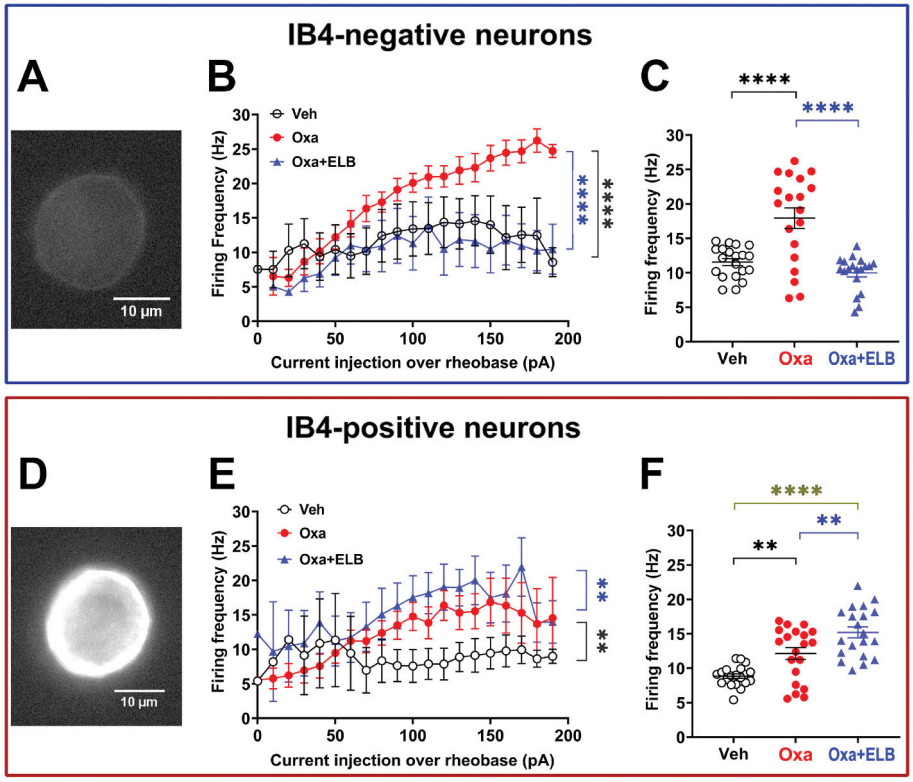

Fig. 4. Opposing effect of ELB00824 on oxaliplatin-induced hyperexcitability in IB4$^-$ and IB4$^+$ DRG neurons.

Oxaliplatin-induced hyperexcitability was characterized *in vitro* in IB4$^-$ (A-C) or IB4$^+$ (D-F) DRG neurons. (A and D) Examples of Alexa-488-conjugated IB4 immunoreactivity in IB4$^-$ (A) or IB4$^+$ (D) neurons. (B and E) Firing frequency as a function of the injected current in the range of 0–200 pA in 10-pA pulses for IB4$^-$ (B) or IB4$^+$ (E) neurons exposed to the following 3 different treatment. (C and F) Firing frequencies from figures B and E, respectively, were plotted as a function of the following 3 treatment groups. Veh: vehicle, Oxa: oxaliplatin 1 h pre-treatment *in vitro*. Oxa + ELB: Oxaliplatin pre-treatment + 10 μM ELB0024 combined pre-treatment for 1 h *in vitro*. Number of neurons from 6 naïve male mice were as follows: Veh, n = 8 (B-C) or 7 (E-F); Oxa, n = 5 (B-C) or 9 (E-F), Oxa + ELB, n = 5 (B-C) or 7 (E-F). Comparison of data from plot. Symbols at mean and error bars at standard error of the mean (SEM) were plot. **p < 0.01, ***p < 0.0001, ****p < 0.0001, ANOVA with Tukey's multiple comparisons test. In figure D and G, pairwise comparison between Oxa group and Oxa + ELB group is indicated with blue line, and that between Oxa group and Veh group is indicated with black line. (For interpretation of the references to colour in this figure legend, the reader is referred to the web version of this article.)

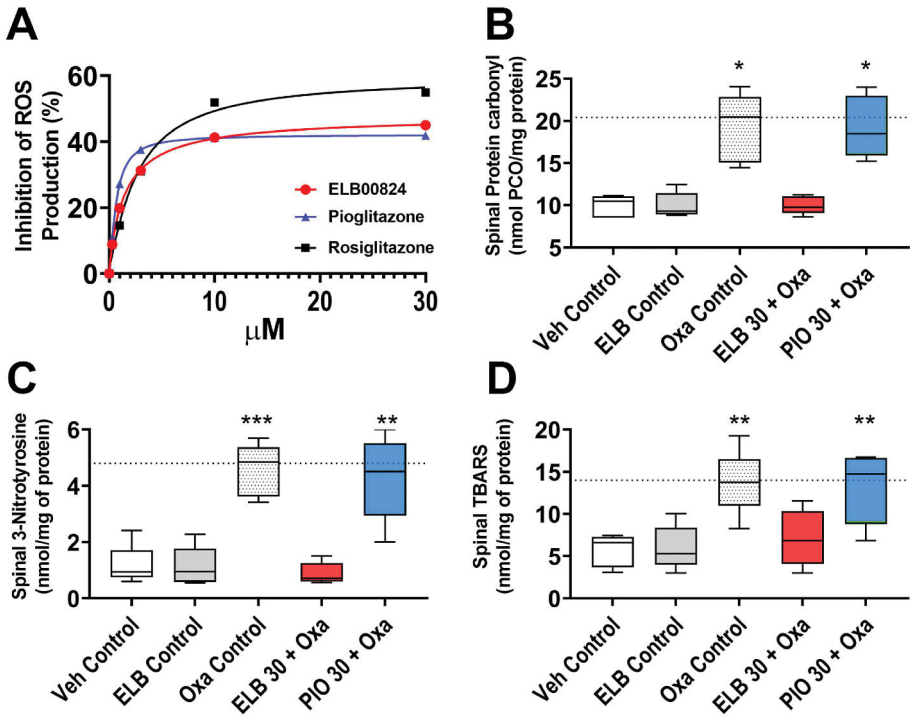

Fig. 5. ELB00824 reduces oxaliplatin-induced oxidative stress in HEK cells and in the spinal cord.

(A)The anti-oxidative effect of ELB00824 was identified *in vitro*, where PPARγ agonists (ELB00824, rosiglitazone, pioglitazone), concentration dependently inhibit ROS production in HEK 293 T cell lines. Data shown are representative of three independent experiments with similar results, normalized to control response in each case (mean ± SD), and fitted using a sigmoidal dose–response curve (Sigmoidal, Sigmoid, 4 Parameter). (B-D) The CNS specific anti-oxidative effect was further confirmed with lumbar spinal cords dissected out from the mouse treatment groups at the end of oxaliplatin treatment period. ELB00824 normalizes oxaliplatin-induced increase in spinal oxidative stress indicated by the levels of the byproducts of protein oxidation (carbonyl level in B, 3-Nitrotyrosine level in C), and lipid peroxidation [Thiobarbituric acid reactive substances (TBARS) level in D]. The box-and-whiskers plots (B-D) show minimum, maximum, median and 25th and 75th percentiles. Inter-group comparison used one-way ANOVA, followed by Dunn's test. *: $p \leq 0.05$; **: $p \leq 0.01$; ***: $p \leq 0.001$ vs Veh Control group. Dashed line is the mean value of Oxa control group at the end of oxaliplatin treatment period in chronic OIPN model.

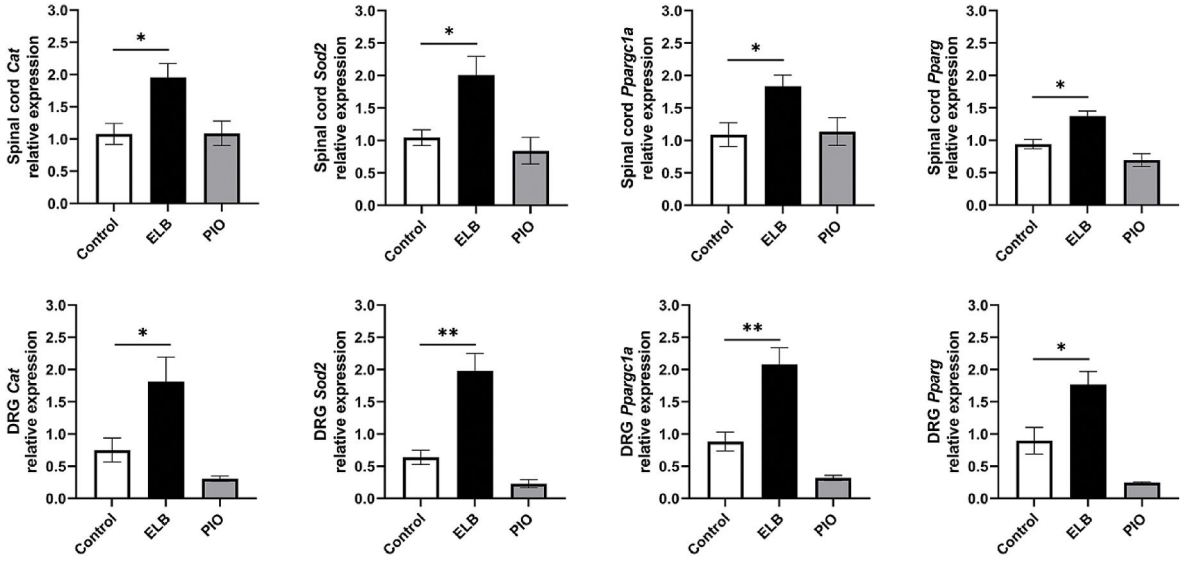

Fig. 6.

ELB00824 effect on genes related to oxidative stress Relative genes expression on Spinal cord and DRG isolated from mice treated 5 consecutive days with oxaliplatin (Control), oxaliplatin + ELB (30 mg/kg), or oxaliplatin + Pioglitazone (PIO, 30 mg/kg), measured by qRT-PCR. Bars represent fold change relative to *Gapdh* (mean ± SEM) for each gene expression in DRG or spinal cord. One-way ANOVA revealed a significant difference between Control and oxaliplatin + ELB; *$p < 0.05$, **$p < 0.005$.

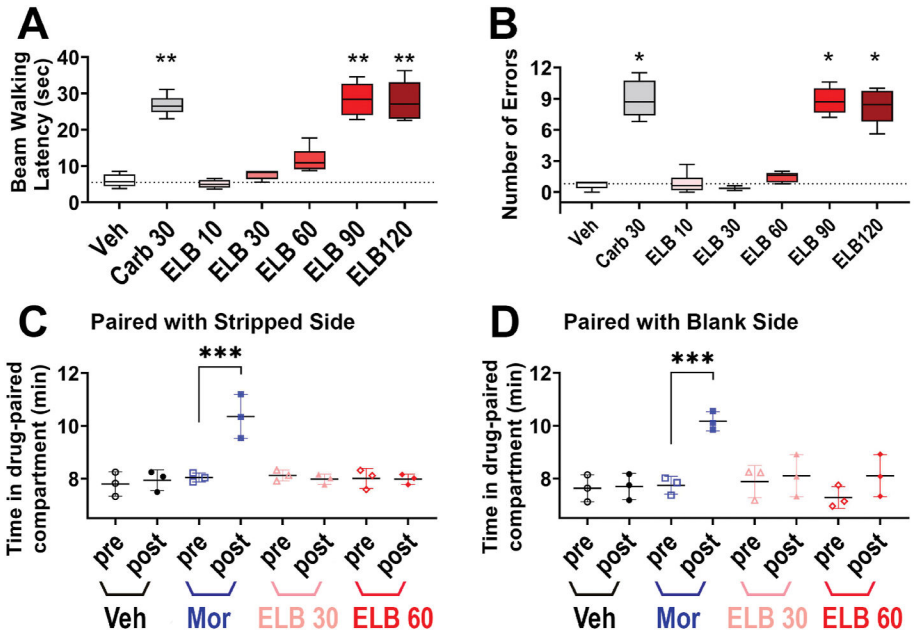

Fig. 7. The CNS safety assessments of ELB00824.

(A and B) The effect of ELB00824 on motor coordination/sedation evaluated by means of beam traversal test, and bars are beam walking latency A in sec) and number of errors (B) committed for the animals (n = 6/group), 2 h after i.p. injection of Veh (DMSO/Cremophor vehicle), Carb 30 (30 mg/kg of carbamazepine), ELB 10, ELB 30, ELB 60, ELB 90, or ELB 120 (10, 30, 60,90, 120 mg/kg of ELB00824, respectively). The box-and-whiskers plots show minimum, maximum, median and 25th and 75th percentiles. Inter-group comparison used one-way ANOVA, followed by Dunn's test. *: $p < 0.05$; **: $p < 0.01$ vs Veh group. (C and D) The effect of ELB00824 on addiction evaluated by conditioned place preference. To pair the drug with one of two distinct contexts, each group was assigned a 'side' of the addiction box: striped (C) or blank (D), and scatter plots are time spent (in min, mean ± SD, n = 3/group) in the drug-paired compartment in the pre-conditioning (pre) and the post-conditioning (post) test sessions on each group on the 2nd day after 3 consecutive daily i.p. injections of either Veh (DMSO/Cremophor vehicle), Mor (5 mg/kg of morphine), ELB 30 (30 mg/kg of ELB00824), or ELB 60 (60 mg/kg of ELB00824). ***$p < 0.001$.

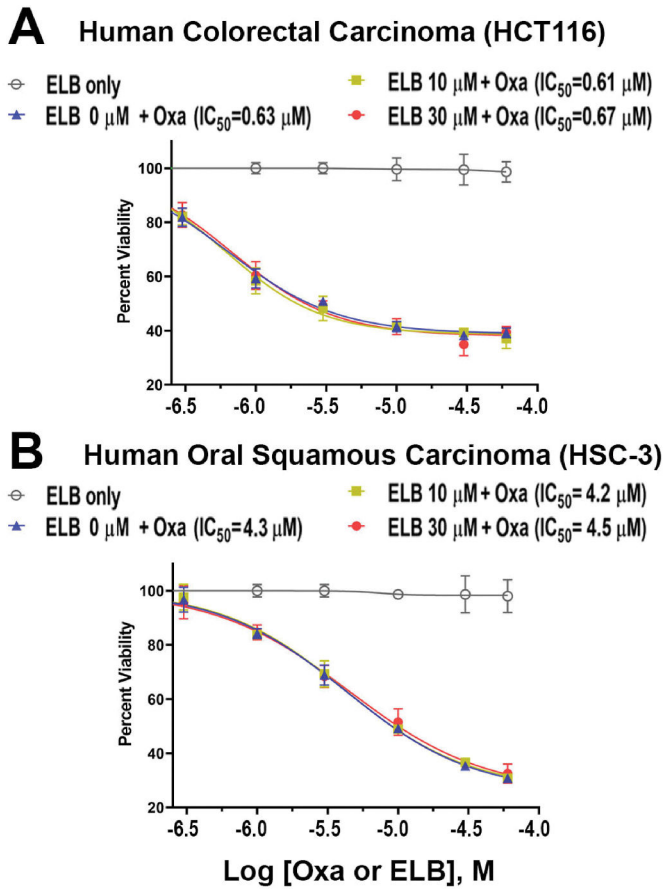

Fig. 8. The effect of ELB00824 on the inhibitory effect of oxaliplatin on cancer cell proliferation.

Human colorectal carcinoma cells (HCT116) in A or Human oral squamous carcinoma cells (HSC-3) in B were incubated 48 h with ELB (ELB00824) only, or with both oxaliplatin (0, 0.3, 1, 3, 10, 30, or 60 μM) and ELB00824 (0, 10, or 30 μM). The viable cell count (%) was determined using the CellTiter-Glo Luminescent Cell Viability Assay. Each plot represents the mean of three wells. IC_{50} is a quantitative measure that indicates the concentration of oxaliplatin is needed to inhibit cell viability by 50%.